

# Adaptive Wideband Aeroacoustic Array Processing

Tien Pham & Brian M. Sadler  
Army Research Laboratory  
Adelphi, MD 20783-1197  
tpham@arl.mil

## ABSTRACT

Incoherent and coherent wideband array processing techniques for aeroacoustic detection and tracking of ground vehicles are contrasted. Experimental results for a circular array are presented, illustrating complexity and performance tradeoffs. Incoherent and coherent MUSIC are used for comparison. Complexity is dominated in both cases by singular value decomposition (SVD) calculation performed  $M$  times for the incoherent case and  $S$  times for the coherent case, where  $M$  is the number of frequency bins and  $S$  is the number of look angles. Good results are obtained with the incoherent method for small  $M$  provided adequate narrowband SNR is available. The coherent approach is more statistically stable, and  $S$  can be reduced by employing a priori coarse direction estimates.

## 1. Introduction

We contrast coherent and incoherent wideband array processing techniques for aeroacoustic detection and tracking of ground vehicles. Experimental results for a circular array of 6 sensors plus 1 at the array center are presented, illustrating complexity and performance tradeoffs in coherent versus incoherent processing.

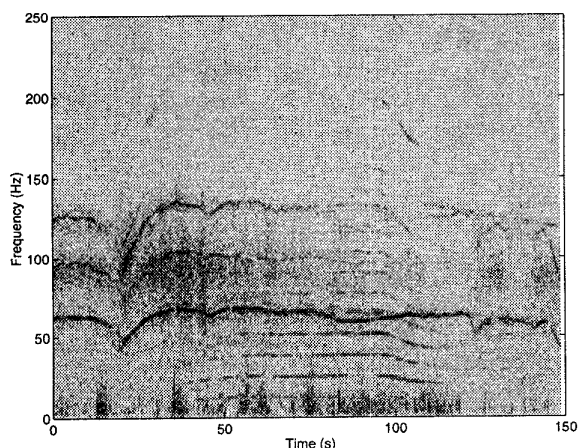


Figure 1. Spectrogram of a ground vehicle and helicopter.

In this application, array baselines are physically constrained by system requirements and variable spatial coherence, motivating use of super-resolution methods [1]. The problem is made difficult by a number of factors. Source acoustic signatures are generally nonstationary and undergo severe fading. The usable

channel is largely restricted to [20,200] Hz due to wind noise at low frequencies and poor propagation at higher ones. The channel response is generally nonstationary due to a variety of atmospheric and terrain factors. There may also be significant time-varying multipath.

A typical spectrogram of a moving vehicle at close range, with a helicopter flying nearby, is shown in figure 1. The helicopter's signature consists of sharp and stable harmonics emanating from the main rotor blade. These are evident in the time interval 50-100 seconds. The ground vehicle also exhibits a harmonic structure but it is very nonstationary and exhibits strong fades during vehicle maneuvering. Note the lack of acoustic energy beyond 200 Hz. The combined effects of source and channel nonstationarities produce significant signal variability, even at relatively close ranges of hundred of meters.

## 2. Incoherent and Coherent Processing

A natural extension of narrowband high resolution subspace methods is to combine narrowband beampatterns over many temporal frequencies [2]. This approach is useful for aeroacoustics if there is sufficient SNR in multiple frequency bins, such that narrowband methods such as MUSIC yield good results independently for each bin. In addition to the relatively high narrowband SNR requirement, disadvantages of this *incoherent* approach include degradation in the presence of correlated multipath, and a general lack of statistical stability when compared to wideband coherent methods. The incoherent averaging can lead to false peaks in the resulting averaged beampattern.

To overcome the nonstationary nature of the source, the data is segmented before processing into fixed blocks, and stationarity is assumed over each block. We have found that this is a reasonable assumption for intervals on the order of 1 sec. Over each processing interval it is assumed that a single frequency bin is occupied by a single source only. This takes advantage of the nonstationarity of the sources, and simplifies the algorithmic complexity as well as estimation of the number of sources. This assumption is justified because different wideband sources are not likely to occupy all of the same bins in any given processing interval, and change bins as a function of time. In practice, the direction of arrival (DOA) estimates are fed into a

tracker that is reasonably robust and therefore able to fill in missing or remove outlying data.

Wideband *coherent* processing gain is possible using the steered covariance method (STCM) originated by Wang and Kaveh [3,4]. STCM is based on forming the composite covariance matrix given by

$$\hat{R}(\theta) = \sum_{m=1}^M T(\omega_m, \theta) \hat{R}_Y(\omega_m) T(\omega_m, \theta)^H \quad (1)$$

where  $M$  is the number of narrowband frequency bins, and  $\hat{R}_Y(\omega_m)$  is the estimated spatial correlation matrix at frequency  $\omega_m$ . The steering or focusing matrix  $T(\omega_m, \theta)$  is a function of both frequency and look angle  $\theta$ . Here it is defined as

$$T(\omega_m, \theta) = \begin{bmatrix} e^{2\pi f_m \Delta t_1} & 0 & \dots & 0 \\ 0 & e^{2\pi f_m \Delta t_2} & \dots & 0 \\ 0 & 0 & \dots & 0 \\ 0 & 0 & \dots & e^{2\pi f_m \Delta t_N} \end{bmatrix} \quad (2)$$

where  $\Delta t_i = \frac{d}{c} \sin \phi_i$ ,  $\phi_i = \theta - \alpha_i$  where  $\alpha_i$  is the relative angle to the normal for sensor  $i$  for  $i=1, 2, \dots, N$ ,  $d$  is the radius of the circular array, and  $c$  is the speed of sound in air. Other forms for  $T(\omega_m, \theta)$  have been suggested to reduce focusing errors. The resulting focused covariance matrix  $\hat{R}(\theta)$  is such that signals in the respective narrowband correlation matrices are mapped into the same subspace, yielding coherent processing gain over multiple frequencies. Conventional subspace methods such as MUSIC can then be applied to  $\hat{R}(\theta)$ , thus requiring eigenanalysis for each  $\theta$ .

The complexity of the coherent approach is increased due to the need for computing  $\hat{R}(\theta)$  for every  $\theta$ . However, the computational load can be lowered by using preliminary estimates of the source locations, obtained, e.g., by conventional beamforming [3]. Also, it is assumed that there is at most a single source for a single look angle  $\theta$ . As we will see, the relative computational complexity between the coherent and incoherent techniques depends on the relative size of the number of look directions versus the number of narrowband frequency bins over which wideband processing occurs.

### 3. Implementation

In this section the processing schemes are described, and estimates of complexity presented for comparing the coherent and incoherent approaches. In both cases MUSIC is used as the means of computing the beampattern. The basic steps are (i) use block-adaptive pre-processing to adaptively select the narrowband frequency bins, (ii) apply incoherent or coherent

techniques, and apply MUSIC, and (iii) estimate the directions of the sources from the resulting beampatterns.

Let  $y_i(n)$  denote the output of the  $i$ th sensor from an array of  $N$  sensors, and let  $Y_i(k)$  denote  $DFT\{y_i(n)\}$ .

The average sum of the  $|Y_i(k)|^2$  is obtained in order to adaptively select frequency bins of interest. This can be performed in a variety of ways, from simple thresholding based on bin SNR, to more complex schemes such as harmonic association. Here, we simply select the  $M$  highest power bins within the range  $\omega_{low}$  to  $\omega_{high}$ .

The conventional narrowband MUSIC beampattern is computed  $M$  times. For each look angle  $\theta$ , we compute

$$P_{Incoh}(\theta) = \sum_{m=1}^M \left[ E(\omega_m, \theta)^H \Pi^\perp(\omega_m) E(\omega_m, \theta) \right]^{-1} \quad (3)$$

where  $E(\omega_m, \theta) = \text{diag}\{T_s(\omega_m, \theta)\}$  is the steering vector and the noise orthonormal projector is defined as

$$\Pi^\perp(\omega_m) = \hat{U}_n(\omega_m) \hat{U}_n(\omega_m)^H. \quad (4)$$

Taking  $\hat{R}_Y(\omega_m)$  to be  $N \times N$  then, by assumption, the noise subspace consists of  $N-1$  eigenvectors corresponding to the  $N-1$  smallest eigenvalues of  $\hat{R}_Y(\omega_m)$ , and these form  $\hat{U}_n(\omega_m)$ .

The computational complexity is approximately  $M[O(N^2) + O(N^3) + S \cdot O(N^2)]$ , where  $M$  is the number of frequency bins and  $S$  is the number of look angles. The first squared term in the bracket corresponds to the formation of the correlation matrix  $\hat{R}_Y(\omega_m)$ , the cubic term is for an SVD calculation to form  $\hat{U}_n(\omega_m)$ , and the last term corresponds to (3) which is computed for each look angle.

The STCM approach requires focusing as a function of look direction. Experimental results shown in the next section are based on computing over 360 degrees in 1 degree steps. After computation of  $\hat{R}(\theta)$  for some angle  $\theta$ , the SVD of  $\hat{R}(\theta)$  yields the unitary noise subspace estimate  $\hat{U}_n(\theta)$ . We assume only one target for each look angle, so that the signal subspace consists of one eigenvector, with the other  $N-1$  eigenvectors forming the noise subspace. The coherent wideband MUSIC spatial-spectrum is then calculated via

$$\hat{P}_{Coh}(\theta) = \left[ L^H \hat{U}_n(\theta) \hat{U}_n(\theta)^H L \right]^{-1} \quad (5)$$

where  $L$  is an  $N$ -element vector of ones.

The computational complexity is approximately  $S[M \cdot O(N^2) + O(N^3) + O(N^2)]$ . The first term in the bracket corresponds to the formation of  $\hat{R}_Y(\omega_m)$  and the focusing operation of (1). Note the diagonal form of  $T(\omega_m, \theta)$  reduces the computation in (1). These

operations must be performed over the range of frequencies ( $M$ ), and the range of look angles ( $S$ ). The cubic term is for the SVD of  $\hat{R}(\theta)$ , and the last term is for calculation of  $\hat{P}_{Coh}(\theta)$  in (5). These are repeated for each look angle, i.e.,  $S$  times.

For both methods, the most expensive computational cost is the SVD which is  $O(N^3)$ . This term tends to dominate the complexity comparison. Note that for the incoherent method it is  $M \cdot O(N^3)$  while for the coherent it is  $S \cdot O(N^3)$ , so that the relative complexity is controlled by the relative size of  $M$  and  $S$ . By assuming a single target for each distinct frequency bin (for incoherent processing) and a single target for each look angle (for coherent processing), we can potentially apply faster eigenanalysis algorithms than the SVD. To reduce the number of frequency bins, harmonic line association techniques can be used to group a set of frequency bins for each source and then only applying MUSIC to the largest narrowband frequency for each set. To reduce the number of look angles  $S$ , coarse angle estimates can be used to narrow the field of view.

#### 4. Experimental results

In this section experimental results for DOA estimation of ground vehicles traveling on a 2 km<sup>2</sup> area of open grass field are presented. For each test run, one of the vehicles was equipped with a GPS sensor to provide accurate positioning ground truth. Figure 2 shows raw experimental DOA estimates, for a single source, for incoherent and coherent wideband MUSIC versus the GPS angles on a test run of 250 seconds in length. Mean square error (MSE) and mean absolute error (MAE) results are shown in table 1 for various sets of  $M$  frequency bins. The  $M$  frequency components are selected based on the highest bin SNR's in the frequency range of [20,200] Hz.

The MSE's and MAE's are calculated with the outliers removed using the criteria

$$|\varepsilon - \text{median}(\varepsilon)| > 3\sigma_{MAD} \quad (8)$$

where  $\varepsilon$  is the angle error or angle difference between the DOA estimate and the true angle measured by GPS, and  $\sigma_{MAD}$  is the mean absolute deviation [5]. An example of this is shown in figure 3, with  $\pm 3\sigma_{MAD}$  shown as straight lines. The outliers can be caused by several factors including fading, wind noise and acoustic source variations. For the error analysis in table 1, the number of outliers ranges from 15 to 24 out of a total of 125 processing intervals of length 1 sec each, sampling rate of 1 kHz, and 1024-pt FFT's. For  $M = 1$ , incoherent and coherent wideband MUSIC reduce to the narrowband case. Processing gain is evident for both

methods, in that the estimates generally improve for increasing  $M$ . For this single source experiment, the incoherent approach produced smaller errors both in terms of MSE and MAE, reflecting the generally high SNR in this experiment.

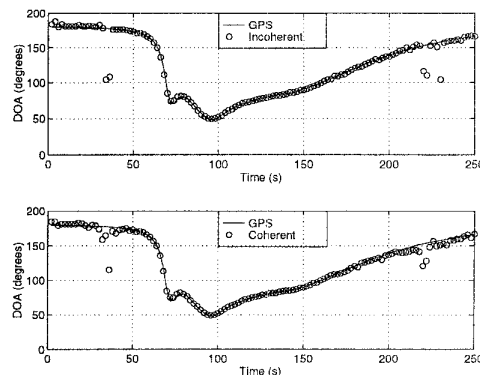


Figure 2: Raw DOA estimates for (a) incoherent and (b) coherent wideband MUSIC for  $M=50$  and GPS ground truth.

$M$	Incoherent MUSIC		Coherent MUSIC	
	MSE	MAE	MSE	MAE
1	3.558	1.419	3.558	1.419
10	2.144	1.083	3.948	1.422
20	1.235	0.870	3.684	1.366
50	1.221	0.863	2.345	1.130
100	1.172	0.838	2.684	1.178

Table 1. MSE and MAE for wideband processing over  $M$  frequency bins between [20,200] Hz.

While the single source, high SNR case can be handled with incoherent MUSIC and small  $M$ , the situation changes with multiple sources and low SNR's. A two-source example is illustrated in figure 4, with sources at 50 and 180 degrees. Here beam patterns are shown for a single processing interval, with  $M$  varying over 10, 20, 50 and 100. The incoherent method accurately locates the directions of the sources for all four cases. It produces more distinct and sharp beam patterns than the coherent method. However, for  $M=50$  (figure 4c) and especially  $M=100$  (figure 4d), the incoherent method produced additional spurious peaks in the beam pattern that can be misconstrued as sources. The explanation for this behavior is that there is high SNR in only a few of the spectral components and no significant SNR elsewhere in the data signature. By incoherently averaging additional beam patterns from low SNR spectral components, the overall beam pattern degrades. The beam pattern for the coherent method on the other hand, becomes more pronounced as  $M$  increases, and exhibits very good statistical stability.

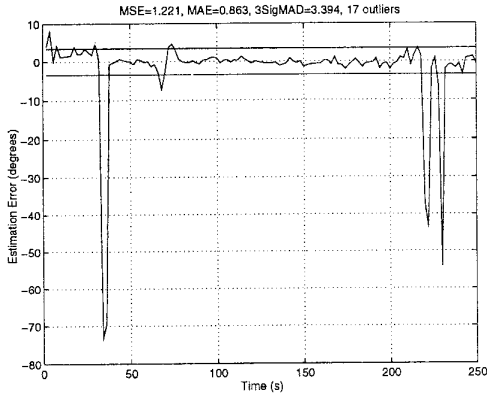


Figure 3: DOA error estimates for incoherent wideband MUSIC ( $M=50$ ) illustrating outlier removal for MSE and MAE calculation.

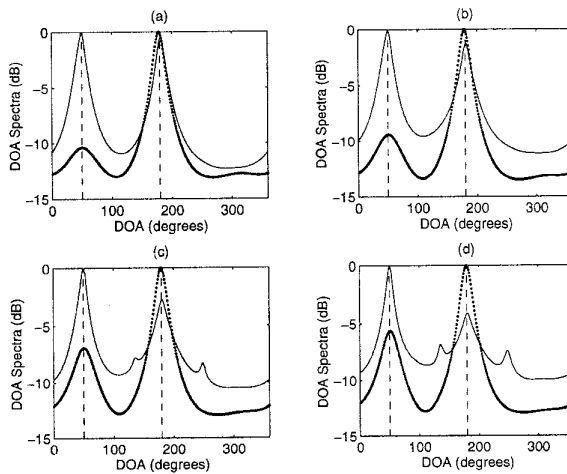


Figure 4: DOA spectra estimates for 2 targets located at  $\theta=50$  and  $\theta=180$  for incoherent (thin line) and coherent wideband MUSIC for (a)  $M=10$  (b)  $M=20$  (c)  $M=50$  and (d)  $M=100$ .

## 5. Conclusions

Both the incoherent and coherent wideband MUSIC methods provide processing gain over narrowband MUSIC, as exhibited by experiment. Here the sources used are generally characterized as a sum of narrowband frequency components for a majority of the time. Thus, given adequate SNR, incoherent MUSIC performed well and yielded sharp and distinct peaks in the beam pattern. However, frequency selection is an issue as the inclusion of low SNR bins tends to degrade the resulting beam pattern, reducing source peaks and introducing spurious ones. In contrast, the coherent MUSIC approach is much more statistically stable, with a beam pattern that generally improves (rather than degrades) with the addition of lower SNR bins. However, the coherent approach requires more frequency bins be included (i.e., larger  $M$ ) to achieve the same accuracy, although this is a function of SNR as well. The

bias introduced in the coherent processing has been ignored, and results in table 1 may partly reflect this fact. It appears that the coherent approach will degrade more gracefully as the SNR is decreased. Thus, further experiments are warranted for lower SNR (longer range) cases, as well as including sources that do not exhibit strong narrowband signatures.

The computational complexity comparison between the two methods is largely governed by the SVD calculation which is  $O(N^3)$ , with a multiplier given by the number of spectral components  $M$  (incoherent) or number of look angles  $S$  (coherent). As we have seen,  $M$  can be made small when the source signatures consist of a sum of high SNR narrowband components, enabling use of the incoherent approach. The number of look angles can be reduced by incorporating coarse DOA estimates obtained in a preprocessing step such as a conventional beamformer. Thus, the complexity of the coherent approach can be made manageable (with respect to the incoherent complexity), and is likely to be warranted for more difficult sources at longer ranges.

It is of interest to consider methods for calculating the signal subspace only, as opposed to the full SVD calculation, because in both methods the signal subspace is assumed to consist of one component only. Further work of interest includes reducing computation by exploiting the radial symmetry of the circular array, e.g., see Doron [6], and effects of calibration and sensor placement errors, e.g., see Swindlehurst [7]. We note that only rudimentary effort was made to calibrate the array used in the experiments.

## 6. References

- [1] T. Pham and B. Sadler, "Aeroacoustic wideband array processing for detection and tracking of ground vehicles," *Journal of the Acoust. Soc. of America*, Vol. 98, No. 5, pt. 2, p. 2969, 1995.
- [2] G. Su and M. Morf, "The signal subspace approach for multiple wide-band emitter location," *IEEE Trans. ASSP*, Vol. 31, No. 6, pp. 1502-1522, December 1983.
- [3] H. Wang and M. Kaveh, "Coherent signal-subspace processing for the detection and estimation of angles of arrival of multiple wideband sources," *IEEE Trans. ASSP*, Vol. 33, pp. 823-831, August 1985.
- [4] J. Krolik, "Focused wideband array processing for spatial spectral estimation," chapt. 6 in *Advances in Spectrum Analysis and Array Processing Vol. II*, S. Haykin ed., Prentice-Hall, 1991.
- [5] L. Ljung, "System Identification for the User," Prentice-Hall, p. 400, 1987.
- [6] M. Doron, E. Doron and H. Weiss, "Coherent wide-band processing for arbitrary array geometry," *IEEE Trans. SP*, Vol. 41, No. 1, pp. 414-417, January 1993.
- [7] A. Swindlehurst and T. Kailath, "A performance based analysis of subspace-based methods in the presence of model errors, part 1: the MUSIC algorithm," *IEEE Trans. SP* Vol. 40, No. 7, pp. 1758-1774, July 1992.